CrystEngComm

PAPER

View Article Online
View Journal | View Issue

Self-assembly patterns of steroid-based all-organic ferroelectrics: valuable insights from the single-crystals derived from an organogel and solution†‡

Cite this: *CrystEngComm*, 2014, **16**, 4861

Deepak Asthana,[a] Sudhir K. Keshri,[a] Geeta Hundal,[b] Gyaneswar Sharma[c] and Pritam Mukhopadhyay*[a]

Received 4th January 2014,
Accepted 28th March 2014

DOI: 10.1039/c4ce00013g

www.rsc.org/crystengcomm

We report herein the first example of a single-crystal grown from a steroid-based organogel matrix. We have delineated the self-assembly process and compared the various non-covalent interactions with that of the single-crystals grown from solution, *e.g.* **1·*Ch*** showed 22 and 14-membered N–H–O H-bonded rings, while **1·*Pr*** exhibited 24 and 14-membered rings. In addition, **1·*Ch*** showed stronger cholesteryl–cholesteryl interactions than **1·*Pr*** and **1·*Ch*** exhibited 55% higher polarization.

Introduction

Ferroelectric (FE) materials have shown attractive applications in FE random-access memory (FERAM), FE diodes, *etc.*[1] FEs are polar materials in which the spontaneous electric polarization can be reversed by inverting the external electric field. It has been realized that all-organic FE materials could provide multi-fold advantages such as synthetic tailorability, tunability of molecular interactions and solution processing compared to the inorganic FEs. However, there are only a very few reported all-organic single-component (AOSC) FE materials.[2] The existing AOSC FE materials suffer from low saturation and remnant electric polarization (P_s and P_r in 10^{-9} C cm^{-2}) and a high E_c value in V cm^{-1}. Two recent reports, based on croconic acid[2b] and a Schiff base,[2c] have shown that exceptional FE properties (P_s ~20–60 μC cm^{-2}) can also be found in AOSC FEs. On the other hand, organic two-component FE systems[3] and metal–ligand based design[4] have been quite successful. In this regard, application of crystal engineering principles would further benefit design of new classes of all-organic FEs.[5,6]

We recently reported the first modular design strategy coupled with a supramolecular[7] self-assembly approach, which leads to ferroelectricity in AOSC crystalline solids as well as in organic nanoarchitectures at RT.[8] The design for molecule **1** incorporates four modules: a donor–π-acceptor module, M_A; a cholesteryl group, M_B; H-bonding groups, M_C; and a spacer, M_D.

1 exhibited remarkable self-assembly properties. It could form stable organogels[9] and could spontaneously gelate acetic acid, carbon tetrachloride and a mixture of various solvents, *e.g.* chloroform : methanol, chloroform : hexane, *etc.* (see the ESI,‡ Table 1). Electron microscopy revealed that these gels consisted of well-defined nanoarchitectures and are dependent on the gelated solvent (Scheme 1a–b). The high propensity to gelate organic solvents created a major challenge to generate good quality single-crystals. After several attempts with different solvents and their combinations we obtained single-crystals by slow evaporation of *n*-propanol (Scheme 1c). These crystals represented as **1·*Pr*** crystallized in the *P*1 polar space group, were found to be second harmonic generation (SHG) active and exhibited spontaneous ferroelectric properties at room temperature (RT).

With these results in hand, we wanted to modulate the self-assembly characteristics by altering the supramolecular interactions. Our goal was to grow single-crystals of **1** in non-polar solvents, albeit the fact that **1** showed strong propensity to gelate non-polar organic solvents. In this work, we demonstrate the successful growth of single-crystals, **1·*Ch***, from an organogel matrix constituted of chloroform and petroleum ether (Scheme 1d–e). To our knowledge this forms the first steroid-based organo-gelator[10] that could be *in situ* crystallized from an organogel matrix.

The single-crystal data for **1·*Ch*** revealed an altered self-assembly pattern, H-bonding interactions, and cholesteryl–cholesteryl van der Waals interactions. The modulation of these supramolecular interactions is anticipated to have a

---

[a] *Supramolecular & Material Chemistry Lab, School of Physical Sciences, JNU, New Delhi, 110067, India. E-mail: m_pritam@mail.jnu.ac.in; Fax: +91 11 26717537; Tel: +91 11 2673 8772*

[b] *Guru Nanak Dev University, Amritsar, India. E-mail: geetahundal@yahoo.com*

[c] *School of Physical Sciences, JNU, New Delhi 110067, India*

† This work is dedicated to Prof. S. Shinkai's 70th birthday.

‡ Electronic supplementary information (ESI) available: CCDC 974686 and 822459. For ESI and crystallographic data in CIF or other electronic format see DOI: 10.1039/c4ce00013g

Table 1 Crystal data for **1**

a) **1·*Ch***		
Empirical formula	$C_{37}H_{56}Cl_3N_3O_4$	
Formula weight	713.20	
Temperature	100(2) K	
Wavelength	0.71073 Å	
Crystal system	Triclinic	
Space group	*P*1	
Unit cell dimensions	a = 13.262(3) Å	α = 76.154(8)°
	b = 13.508(2) Å	β = 86.364(9)°
	c = 24.549(4) Å	γ = 63.763(8)°
Volume	3825.5(12) $Å^3$	
Z	4	
Density (calculated)	1.238 Mg m^{-3}	
Absorption coefficient	0.281 mm^{-1}	
F(000)	1528	
Crystal size	0.21 × 0.16 × 0.10 mm^3	
Theta range for data collection	1.71 to 25.40°	
Reflections collected	50 819	
Independent reflections	24 785 [*R*(int) = 0.0503]	
Refinement method	Full-matrix-block least-squares on F^2	
Data/restraints/ parameters	24 785/20/1717	
Goodness-of-fit on F^2	0.975	
Final *R* indices [$I > 2\sigma(I)$]	R_1 = 0.0628, wR_2 = 0.1517	
R indices (all data)	R_1 = 0.0975, wR_2 = 0.1753	
Absolute structure parameter	−0.04(5)	
Largest diff. peak and hole	0.909 and −0.581 e $Å^{-3}$	
CCDC no. (**1·*Ch***)	974686	
b) CCDC no. (**1·*Pr***)	822459	

significant role in tuning the nonlinear optical (NLO)[11] and FE properties of these materials. Furthermore, significant control over the cholesteryl–cholesteryl interactions in the solid state is important in the design of steroid-based drug molecules.

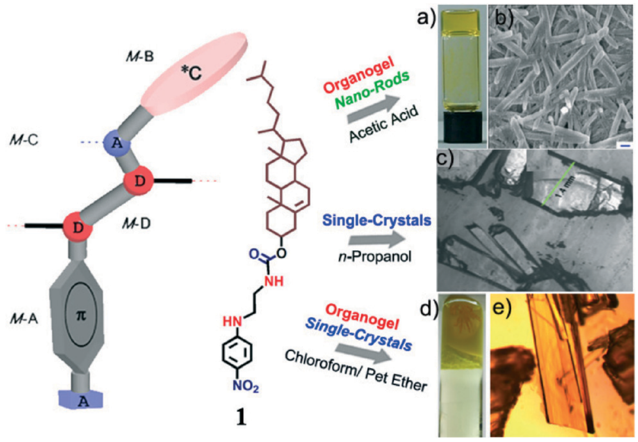

Scheme 1 A module-based design of all-organic ferroelectric **1**; a) organogel formation in acetic acid; b) a SEM image exhibiting the nanorod like structures; c) single-crystals grown from *n*-propanol; d) organogel formation in chloroform : petroleum ether; and e) *in situ* formation of single-crystals from the organogel matrix.

Results and discussion

1·*Ch* crystallizes in the triclinic crystal system with the polar space group *P*1, similar to **1·*Pr***, which comprises one of the ten polar point groups necessary for ferroelectricity to occur (Table 1). There were four crystallographically independent molecules in the unit cell along with four independent chloroform molecules (see the ESI‡ for the thermal ellipsoid plot). The cell dimensions of **1·*Ch*** were slightly elongated and the cell volume was found to be marginally expanded as compared to that of **1·*Pr*** [a = 12.9772(3), b = 14.3714(2), c = 22.6800(6), V = 3779.5(1) $Å^3$].

Self-assembly characteristics

An infinite bi-layer like assembly of the polar nitrophenyl rings (head) and the non-polar cholesteryl groups (tail) in a head–tail–tail–head (H–T–T–H) arrangement could be unravelled in **1·*Ch*** (Fig. 1). In this H–T–T–H arrangement, the two cholesteryl T's interact with the peripheral alkyl chains. In the bilayer, the two nitrophenyl rings are stacked offset to each other and the solvent chloroform molecules are at the periphery of the bilayer and close to the nitrophenyl rings. In the subsequent sections, we would discuss in detail the H-bonding interactions, molecule–solvent interactions, π–π stacking and cholesteryl–cholesteryl interactions.

In **1·*Pr***, a similar H–T–T–H bi-layer like assembly was observed for the *n*-propanol molecules in close proximity to the nitrophenyl rings (Fig. 2). It should be noted that a similar H–T–T–H arrangement of cholesteryl-based molecules has been observed and characterized in detail in liquid crystals.

H-bonding features

In **1·*Ch*** an infinite H-bonded array was observed, formed by the donor NH-groups of *p*-nitroaniline and the amide moiety

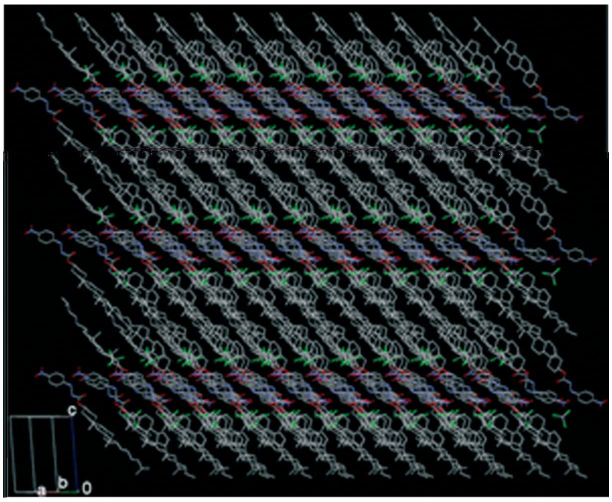

Fig. 1 An infinite bi-layer like arrangement of the polar nitrophenyl rings and the non-polar cholesteryl groups in **1·*Ch***. H atoms have been removed for clarity. Colour code for atoms: C, grey; N, blue; O, red; Cl, green.

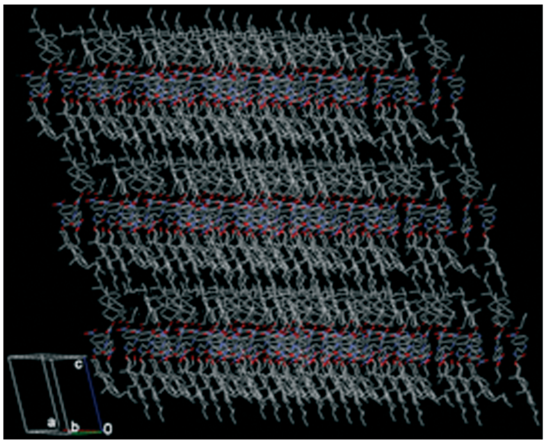

Fig. 2 An infinite bi-layer like arrangement of the polar nitrophenyl rings and the non-polar cholesteryl groups in **1·*Pr***. H atoms have been removed for clarity. Colour code for atoms: C, grey; N, blue; O, red.

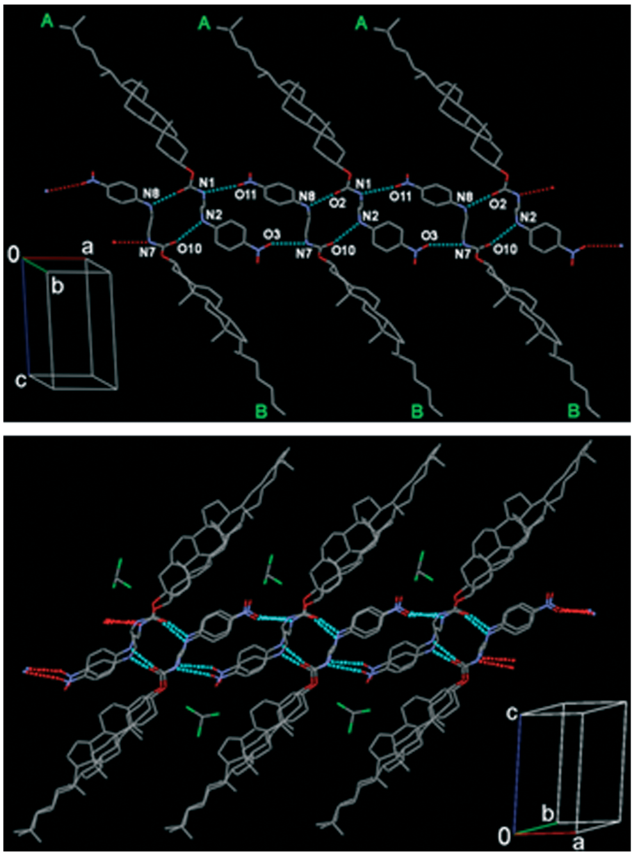

Fig. 3 Top: an infinite array of N–H–O H-bonds in **1·*Ch*** formed by two types of rings, R1 (22-membered) and R2 (14-membered), and H-bonded chains along the *a*-axis. Bottom: an infinite array of N–H–O H-bonds along the *a*- and *c*-axes. Note that the solvent chloroform molecules do not participate in forming the infinite rings and the chains in the H-bonded structure.

and the acceptor O atoms of the nitro-group and the amide moiety. A closer look at the array reveals two types of well-defined rings (R1 and R2) and a chain that aids to achieve the infinite propagation. The bigger H-bonded ring (R1) is subtended by 22 atoms, while the smaller ring (R2) is subtended by 14 atoms (Fig. 3, top panel). In R1, the characteristic H-bonding parameters were found to be: N1–O11 2.959 Å, ∠N1–H1–O11 of 143° and N7–O3 2.954 Å, ∠N7–H7–O3 of 135°, while in R2 the H-bonding parameters were found to be: N8–O2 2.87 Å, ∠N8–H8–O2 of 168° and N2–O10 2.858 Å, ∠N2–H2–O10 of 162°.

The solvent chloroform molecules did not participate in the H-bonded ring and chain formation (Fig. 3, bottom panel). However, a weak C–H–X type of bonding was unravelled between the H atoms of the cholesteryl rings and the Cl atoms, *e.g.* H12b–Cl8 2.775 Å, ∠C12–H12b–Cl8 of 153°; H15a–Cl5 2.847 Å, ∠C15–H15a–Cl5 of 169°, *etc.* (see the ESI‡).

In contrast to **1·*Ch***, the solvent *n*-propanol molecules in **1·*Pr*** participated in forming the infinite H-bonded array. In this case, R1 is subtended by 24 atoms and the additional two atoms (compared to **1·*Ch***) are from the H's of the two propanol molecules. R2 is similar to **1·*Ch*** and is subtended by 14 atoms (Fig. 4, top panel). In ring R2, the notable H-bond distances and angles are: N10c–O49 2.915 Å, ∠N10c–H10c–O49 of 175° and O49–O1d 2.915 Å, ∠O49–H49–O1 of 166°. In R2, the H-bonding parameters were found to be: N7d–O12c 2.893 Å, ∠N7d–H7d–O12c of 158° and N7c–O12d 2.943 Å, ∠N7c–H7c–O12d of 168°.

π–π stacking interactions

The donor–π-acceptor *p*-nitroaniline moiety is stacked in an antiparallel fashion in **1·*Ch*** and **1·*Pr*** single-crystals (Fig. 5). In the case of **1·*Ch*** and **1·*Pr***, the centroid–centroid distances between the two π-rings were found to be 4.316 Å and 3.851 Å. These show a weak π–π stacking interaction in the organogel matrix. In both of these cases the π-rings were found to be tilted, which provides a net dipole to the bulk system as verified by the SHG activity.[8]

Cholesteryl–cholesteryl van der Waals interaction

The cholesteryl moiety is known to play a significant role in the design of soft materials like organogels, liquid crystals,[12] well-defined nanoarchitectures, *etc.* In addition, understanding and control over their interactions play a significant role in modulating the efficacy of steroid-based drug molecules. We are interested in delineating the cholesteryl–cholesteryl interactions in **1·*Ch*** and **1·*Pr*** and arriving at a synthetic toolbox for engineering soft materials.

In the case of **1·*Ch*** several short C–C interactions less than 4.0 Å were observed between the cholesteryl moieties. Notable short interactions were found between C61–C24 (3.515 Å), C47–C21 (3.882 Å), and C99–C114 (3.997 Å). Such short cholesteryl–cholesteryl interactions have been observed in the single crystals of metal cholesteryl–phosphine complexes.[13] In contrast, the cholesteryl–cholesteryl interactions in **1·*Pr*** were found to be much weaker, only one short C–C interaction was observed between C19b–C34d (3.507 Å). Therefore, such

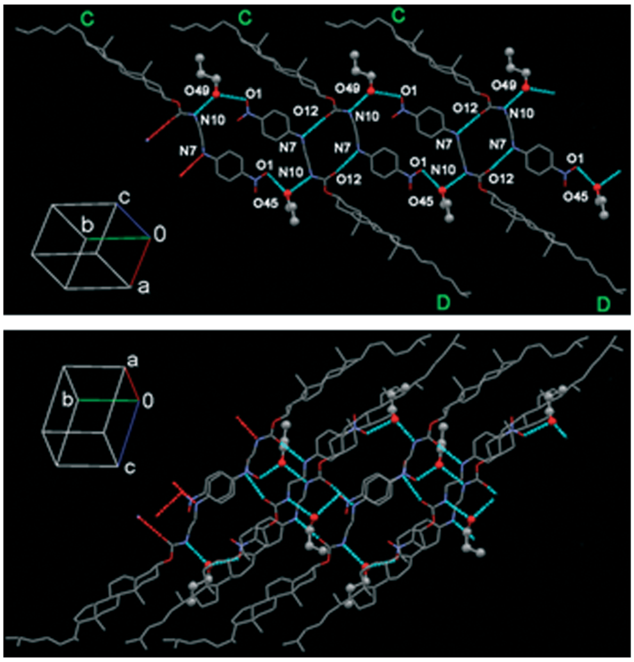

Fig. 4 Top: an infinite array of N–H–O and O–H–O H-bonds in 1·*Pr* formed by two types of rings, R1 (24-membered) and R2 (14-membered), and H-bonded chains along the *b*-axis. Bottom: an infinite array of N–H–O and O–H–O H-bonds along the *a*- and *b*-axes. Note the participation of the solvent propanol molecules (shown in ball and stick representation) in forming the infinite rings and the chains in the H-bonded structure.

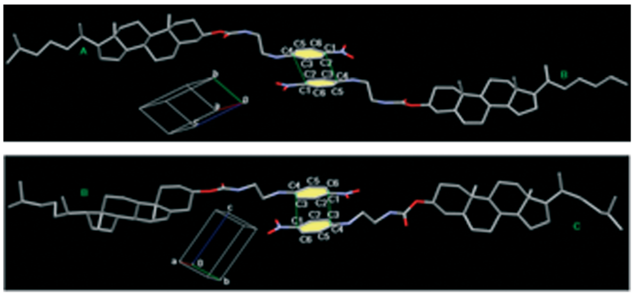

Fig. 5 Top: π–π stacking interactions in 1·*Ch*; bottom: π–π stacking interactions in 1·*Pr*.

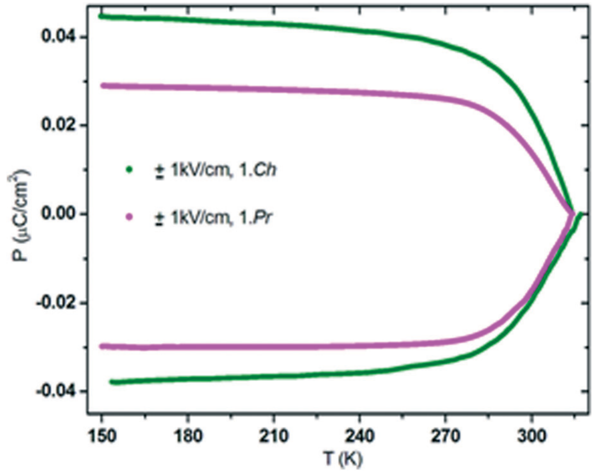

Fig. 6 Graphs showing polarization as a function of temperature (*T*) obtained by pyroelectric current measurement of 1·*Ch* and 1·*Pr*.

solvent dependent modulation of cholesteryl–cholesteryl interactions in a small molecule should be useful in tuning the material properties associated with soft-materials.

Ferroelectric properties

Following the standard procedure,[14] which has been recently used to validate the FE properties of croconic acid,[2b] we studied the FE properties of the crystalline material of 1·*Ch* and compared them with those of the previously reported 1·*Pr*. We determined the temperature dependent changes in polarization by measuring the pyroelectric current during a steady temperature sweep. The pellets were coated with silver paste on both sides and contacts were made using copper wires. The sample was cooled up to 150 K in the presence of an electric field of 100 V (for details, see the ESI‡). It was then heated uniformly up to 310 K at a constant rate and the current was measured as a function of temperature using an electrometer. The observed pyroelectric current during the heating process was integrated with time to obtain the change in spontaneous polarization (Fig. 6). As expected, the polarization gradually decreased with the increase of the temperature. Comparing the results from these two sets of experiments, we found that the polarization value for 1·*Ch* (0.045 μC cm^{-2}) is 55% higher compared to that of 1·*Pr* (0.029 μC cm^{-2}).[14b] This can be attributed to higher asymmetry in molecular packing and also to the resultant higher dipoles emerging from 1·*Ch*. A closer look at Fig. 3 (top and bottom panels) clearly shows that the donor–π-acceptor *p*-nitroaniline moiety in 1·*Ch* has a greater tilt angle compared to 1·*Pr* (Fig. 4) and hence, leading to the increase in the net dipole in 1·*Ch*.

Conclusions

In conclusion, we have provided the first crystallographic snapshots of molecular interactions of a steroid-based all-organic ferroelectric material. To the best of our knowledge, this is the first example of a single-crystal (1·*Ch*) grown from a steroid-based organogel matrix. We have delineated the self-assembly process by delving into the H-bonding patterns, π–π and cholesteryl–cholesteryl interactions and also the solvent (chloroform) interaction mode with 1. Furthermore, we compared these non-covalent interactions with that of the single-crystals grown from *n*-propanol solution, *e.g.* 1·*Ch* showed 22 and 14-membered N–H–O H-bonded rings, while 1·*Pr* exhibited 24 and 14-membered rings formed from the combination of N–H–O and O–H–O H-bonds. In addition, 1·*Ch* demonstrated a stronger cholesteryl–cholesteryl interaction compared to 1·*Pr*. These provide valuable insights into modulating these interactions and tuning the optical and electronic properties of soft materials. We determined the temperature dependent changes in polarization by measuring the pyroelectric current during a steady temperature sweep. **1**·***Ch*** exhibited higher polarization compared to **1**·***Pr*** as a result of higher asymmetry in molecular packing and the emergent net dipole.

Experimental

Materials and methods

All chemicals were obtained from Sigma Aldrich or Spectrochem India and were used as received. Thin layer chromatography (TLC) was carried out on aluminium plates coated with silica gel mixed with a fluorescent indicator having a particle size of 25 μm and was sourced from Sigma Aldrich. ^{1}H and ^{13}C NMR spectra were recorded using a Bruker 500 MHz spectrometer in DMSO-d_6 with TMS as the standard. Infrared spectra were recorded in a KBr pellet using a Varian 3100 FT-IR instrument. The morphologies of the xerogels were investigated using a field emission scanning electron microscope (FE-SEM) apparatus (JEOL, JSM-6700F). The samples were platinum coated with a thickness of 40 nm by a sputtering technique in an argon atmosphere and were observed at a voltage of 5 kV.

Synthetic procedures

The detailed synthetic procedure for **1** is given in the ESI.‡

In situ growth of single-crystals of **1** from the organogel matrix: 30 mg of **1** was dissolved in 0.5 ml of $CHCl_3$ and then petroleum ether (4-times by volume) was added slowly from the top. A turbid layer was formed and the vial was closed and kept at room temperature. The chloroform layer and some part of the petroleum ether layer turned into a gel. After around 6–7 days single-crystals were formed in the organogel matrix.

Crystallography

The structure of **1** was refined by a blocked diagonal refinement procedure as the number of parameters was high since there were four crystallographically independent molecules in the unit cell along with four independent chloroform molecules. All non-hydrogen atoms were refined anisotropically. All calculations were performed using the WinGX package.[15] The amide hydrogens in the structure were located by the difference Fourier synthesis and were refined isotropically with U_{iso} values 1.2 times those of the carrier nitrogen atoms, with a fixed distance [0.88(2) Å] wherever needed.

Ferroelectric properties

The experiments were performed in a pellet form. The pellets were obtained by applying 3.0–3.5 ton of pressure under a hydraulic pellet press. The pellets were coated with silver paste on both sides and contacts were made using copper wires. The sample was cooled up to 150 K in the presence of an electric field of 100 V. After removing the applied field, the sample was short-circuited to avoid the influence of the charge stored during the process of poling for 10 minutes to remove the possibility of any stray charge. The sample was then heated uniformly up to 310 K at a constant rate and the current was measured as a function of temperature using a Keithle-6514 system electrometer.

Acknowledgements

We thank the DBT-BUILDER and the DST-PURSE for funding this research. We thank the MALDI-TOF MS, FT-IR, and 500 MHz NMR facilities at AIRF, JNU. DA thanks the CSIR, India, for the research fellowship. We acknowledge Dr. S. Patnaik, SPS, JNU for providing the experimental facilities for the ferroelectric studies.

References

1 (*a*) S. J. Kang, I. Bae, Y. J. Park, T. H. Park, J. Sung, S. C. Yoon, K. H. Kim, D. H. Choi and C. Park, *Adv. Funct. Mater.*, 2009, **19**, 1609; (*b*) R. C. G. Naber, K. Asadi, P. W. M. Blom, D. M. De Leeuw and B. de Boer, *Adv. Mater.*, 2009, **21**, 1; (*c*) R. Schroeder, L. A. Majewski and M. Grell, *Adv. Mater.*, 2004, **16**, 633; (*d*) F. Kagawa, S. Horiuchi, M. Tokunaga, J. Fujioka and Y. Tokura, *Nat. Phys.*, 2010, **6**, 169; (*e*) G. Rogez, N. Viart and M. Drillon, *Angew. Chem., Int. Ed.*, 2010, **49**, 1921.

2 For single component organic ferroelectric solids, see: (*a*) J. Valasek, *Phys. Rev.*, 1921, **17**, 475; (*b*) S. Horiuchi, Y. Tokunaga, G. Giovannetti, S. Picozzi, H. Itoh, R. Shimano, R. Kumai and Y. Tokura, *Nature*, 2010, **463**, 789; (*c*) Y. Sui, D.-S. Liu, R.-H. Hu and H.-M. Chen, *J. Mater. Chem.*, 2011, **21**, 14599; (*d*) J. Sapriel, A. Boudou and A. Perigaud, *Phys. Rev. B: Condens. Matter Mater. Phys.*, 1979, **19**, 1484; (*e*) P. Szklarz and G. Bator, *J. Phys. Chem. Solids*, 2005, **66**, 121; (*f*) P.-B. Gruner and E. Dormann, *J. Phys.: Condens. Matter*, 1992, **4**, 5599; (*g*) Y. Kamishima, Y. Akishige and M. Hashimoto, *J. Phys. Soc. Jpn.*, 1991, **60**, 2147.

3 For two-component organic ferroelectric solids, see: (*a*) S. Horiuchi and Y. Tokura, *Nat. Mater.*, 2008, **7**, 357; (*b*) S. Horiuchi, R. Kumai and Y. Tokura, *Chem. Commun.*, 2007, 2321.

4 For organic–inorganic hybrid ferroelectric solids, see: (*a*) T. Okubo, R. Kawajiri, T. Mitani and T. Shimoda, *J. Am. Chem. Soc.*, 2005, **127**, 17598; (*b*) Q. Ye, Y.-M. Song, G.-X. Wang, K. Chen, D.-W. Fu, P. W. H. Chan, J.-S. Zhu, S. D. Huang and R.-G. Xiong, *J. Am. Chem. Soc.*, 2006, **128**, 6554; (*c*) W.-W. Zhou, J.-T. Chen, G. Xu, M.-S. Wang, J.-P. Zou, X.-F. Long, G.-J. Wang, G.-C. Guo and J.-S. Huang, *Chem. Commun.*, 2008, 2762; (*d*) W. Zhang, R.-G. Xiong and S. D. Huang, *J. Am. Chem. Soc.*, 2008, **130**, 10468.

5 (*a*) G. R. Desiraju, *Angew. Chem., Int. Ed.*, 2007, **46**, 8342; (*b*) G. R. Desiraju, *Angew. Chem., Int. Ed. Engl.*, 1995, **34**, 2311.

6 (*a*) P. Dastidar, *Chem. Soc. Rev.*, 2008, **37**, 2699; (*b*) D. R. Trivedi, A. Ballabh and P. Dastidar, *CrystEngComm*, 2003, **5**, 358; (*c*) D. K. Kumar, D. A. Jose, A. Das and P. Dastidar, *Chem. Commun.*, 2005, 4059.

7 J.-M. Lehn, *Supramolecular Chemistry: Concepts and Perspectives*, Wiley-VCH, Weinheim, 1995.

8 D. Asthana, A. Kumar, A. Pathak, P. K. Sukul, S. Malik, R. Chatterjee, S. Patnaik, K. Rissanen and P. Mukhopadhyay, *Chem. Commun.*, 2011, **47**, 8928.

9 Organogels: (*a*) S. Banerjee, R. K. Das and U. Maitra, *J. Mater. Chem.*, 2009, **19**, 6649; (*b*) D. K. Smith, *Chem. Soc. Rev.*, 2009, **38**, 684; (*c*) N. Fujita, P. Mukhopadhyay and S. Shinkai, *Annu. Rev. Nano Res.*, 2006, **1**, 385.

10 Steroid based smart organogels: (*a*) S.-I. Kawano, N. Fujita and S. Shinkai, *Chem. – Eur. J.*, 2005, **11**, 4735; (*b*) M. Numata and S. Shinkai, *Chem. Lett.*, 2003, **32**, 308; (*c*) Y. Iwashita, K. Sugiyasu, M. Ikeda, N. Fujita and S. Shinkai, *Chem. Lett.*, 2004, **33**, 1124; (*d*) E. Ostuni, P. Kamaras and R. G. Weiss, *Angew. Chem., Int. Ed. Engl.*, 1996, **35**, 1324.

11 (*a*) P. Mukhopadhyay, P. K. Bharadwaj, G. Savitha, A. Krishnan and P. K. Das, *Chem. Commun.*, 2000, 1815; (*b*) P. Mukhopadhyay, P. K. Bharadwaj, A. Krishnan and P. K. Das, *J. Mater. Chem.*, 2002, **12**, 2786.

12 S. T. Lagerwall, *Ferroelectric and Antiferroelectric Liquid Crystals*, Wiley-VCH, Weinheim, 1999.

13 R. Deschenaux, M. Even and D. Guillon, *Chem. Commun.*, 1998, 537.

14 (*a*) M. E. Lines and A. M. Glass, Principles and Applications of Ferroelectrics and Related Materials, *Oxford Classic Texts in the Physical Sciences*, 2001; (*b*) The magnitude of the polarization, *P*, determined by the polarization–temperature (P–T) sweep method and the P–E loop method is not comparable. In the P–T experiments, lower fields are applied and hence fewer domains get aligned.

15 L. J. Farrugia, *J. Appl. Crystallogr.*, 1999, **32**, 837.